

Programmed Metalloporphyrins for Self-Assembly within Light-Harvesting Stacks: (5,15-Dicyano-10,20-bis(3,5-di-*tert*-butylphenyl)porphyrinato)zinc(II) and Its Push–Pull 15-*N,N*-Dialkylamino-5-cyano Congeners Obtained by a Facile Direct Amination

Mihaela Carmen Balaban,[†] Andreas Eichhöfer,[†] Gernot Buth,[‡] Robert Hauschild,^{||} Jędrzej Szymtkowski,^{||} Heinz Kalt,^{||} and Teodor Silviu Balaban^{*,†}

Karlsruhe Institute of Technology (KIT), Forschungszentrum Karlsruhe (FZK), Institute for Nanotechnology (INT), and Institute for Synchrotron Radiation (ISS), Postfach 3640, D-76021 Karlsruhe, Germany, Faculty for Applied Physics, Universität Karlsruhe (UKA), Karlsruhe, Germany, and Center for Functional Nanostructures (CFN), Universität Karlsruhe, Germany

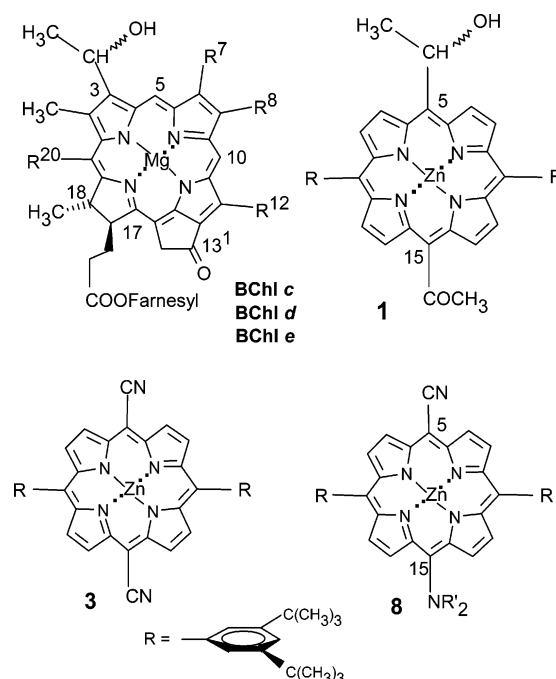
Received: February 20, 2008

The title dicyano compound was synthesized via cyanation and it self-assembles in nonpolar solvents giving red-shifted and broad absorption maxima just as the bacteriochlorophylls which are encountered in the light-harvesting organelles of early photosynthetic bacteria. In the crystal, stacks are formed through a hierarchic combination of π -stacking and a CN–Zn electrostatic interaction. Push–pull 15-*N,N*-dialkylamino-5-cyano congeners could be obtained in high yields using a solvent- and catalyst-free direct amination of *meso*-bromoporphyrins. Importantly, the fluorescence of the self-assembled species due to the very orderly manner in which the chromophores are arranged is not entirely quenched and has a surprisingly long lifetime of over 1 ns. This lends hope of using the trapped energy in biomimetic hybrid solar cells.

Introduction

Early green photosynthetic bacteria have developed a unique organelle for light-harvesting in deep waters where they can scavenge photons even at 100 m under the water surface.¹ Recently, an oceanic microbe living at a depth of 2390 m, near a volcanic vent, was identified to harvest infrared radiation and thus is obligatory photosynthetically active in the absence of solar radiation.² The antenna organelles of these green bacteria are different from the light-harvesting complexes of for instance purple bacteria, cyanobacteria, algae, or plants where proteins organize the photoactive pigments such as (bacterio)chlorophylls, [(B)Chl]s, and carotenoids into precise orientations enabling an energy funneling from the peripheral antenna systems to the core where charge separation occurs within the reaction center.³ Because of their much simpler genomes, these bacteria can avoid using a protein scaffold by self-assembling BChl *c*, *d*, and *e* forming nanostructures called chlorosomes (from Greek “green sacs”) with a large photon capture cross section.⁴ In spite of considerable research efforts, in the absence of crystallographic proof, the exact chlorosomal structure remains elusive and several models have been proposed recently.⁵ We could replicate the BChl self-assembly with fully synthetic chromophores, such as porphyrins and chlorins, by appending to them the same functional groups capable of forming supramolecular interactions.⁶ Tamiaki⁷ and Würthner⁸ have used semisynthetic approaches starting from Chl *a* to prepare after self-assembly functional antenna systems. In all these cases, a hydroxy group, a central metal atom within the tetrapyrrolic core, and a carbonyl group were present in the constructs. Using the very versatile 3,5-di-*tert*-butylphenyl group

CHART 1: BChls and Their Mimic 1 Together with the New Compounds 3 and 8 Addressed in This Work^a



^a In bacteria, BChls are present as mixtures of *R*⁸ and *R*¹² homologues (Me, Et, *n*Pr, *i*Bu) as well as *R/S* epimers of the 3¹ stereocenter. Farnesol is the most frequently encountered fatty alcohol esterifying the 17-propionic acid residue. Stearol, cetol, geranyl–geraniol, and phytol are other such hydrophobic alcohols. In BChl *c*, *R*⁷ and *R*²⁰ are both CH₃ groups. In BChl *d*, *R*⁷ is CH₃ while *R*²⁰ is H. In BChl *e*, *R*⁷ is CH=O while *R*²⁰ is CH₃.

as solubilizing moiety, but which at the same time packs well into the crystal lattice, we could recently crystallize two assemblies of the zinc porphyrin **1**.⁹ Contrary to all previously

* To whom correspondence should be addressed. Fax: +49-724-782-8298. E-mail: silviu.balaban@int.fzk.de; silviu.balaban@kit.edu.

[†] KIT, FZK, INT, and CFN.

[‡] KIT, FZK, ISS.

^{||} KIT, UKA, and CFN.

proposed chlorosomal models, no hydrogen bonds exist within the crystal lattices of **1**. Stacks are formed by a strong Zn–OH ligation and π – π interactions, while the carbonyl group is involved in a weak electrostatic Zn–O=C< interaction, with ~ 3.5 Å Zn to oxygen spacing which is beyond a usual supramolecular bonding distance. The carbonyl group is therefore unavailable for hydrogen bonding.⁹

Materials and Methods

General Remarks. Solvents were dried by prolonged heating under reflux (dichloromethane over calcium hydride, toluene and tetrahydrofuran over sodium benzophenone ketyl, *n*-heptane over sodium metal), freshly distilled under nitrogen, and freed from any residual oxygen by passing a flow of dry nitrogen for 3 min. The solvents for chromatography were sonicated shortly before use. All reactions flasks and chromatography columns were protected from ambient light with aluminum foil. Reactions were performed under nitrogen or argon atmosphere. NMR spectra were recorded at 300 MHz (for ¹H) with a Bruker DPX 300 Avance spectrometer. Chemical shifts are given in ppm relative to the signal of CHCl₃, which was taken as $\delta = 7.26$ (for ¹H) and 77.00 (for ¹³C). Coupling constants are given in Hz. UV/vis spectra were measured with a Varian Cary 500 equipped with a Peltier variable-temperature unit. Fluorescence spectra were measured on a Varian Eclipse fluorometer. MALDI-ToF spectra were obtained on a Voyager Instrument from Applied Biosystems with 1,8,9-anthracenetriol as matrix. HR-FAB-MS results were recorded using 3-nitrobenzyl alcohol (NBA) as a matrix on a Finnigan MAT 90 machine. Column chromatography was performed with Merck silica gel 0.040–0.063 nm. Retention factors are given for silica gel TLC plates (Macherey Nagel silica gel Polygram SIL 6/UV₂₅₄) using dichloromethane (0.2% ethyl alcohol as stabilizing agent) unless otherwise specified.

(5,15-Dicyano-10,20-bis(3,5-di-*tert*-butylphenyl)porphyrinato)zinc(II) (3). 5,15-Dibromo-10,20-bis(3,5-di-*tert*-butylphenyl)porphyrin free base (**2**)¹⁰ (100 mg, 0.12 mmol), tris(dibenzylideneacetone)dipalladium (Pd₂(dba)₃, 32.5 mg, 0.035 mmol, 30 mol %), 1,1'-bis(diphenylphosphino)ferrocene (dppf, 39 mg, 0.07 mmol, 60 mol %), activated zinc powder (7 mg, 0.1 mmol, 90 mol %), and anhydrous zinc cyanide (22 mg, 0.19 mmol, 160 mol %) were weighed under nitrogen atmosphere and filled as solids in an overnight oven-dried (at 111 °C) 50 mL flask. Anhydrous *N,N*-dimethylacetamide (DMA, 12 mL) purchased from Aldrich was degassed by passing a flow of argon for 3 min and was cannulated to the reaction flask which was then heated under magnetic stirring at 120 °C for 4 h under a dry nitrogen atmosphere. After the temperature reached 120 °C, usually a deep pine tree green color was observed. With smaller catalyst loading (e.g., 4 mol %), the induction period is longer and the reaction can be triggered by adding fresh Pd₂(dba)₃, dppf, and activated zinc (without zinc cyanide) with up to 30 mol % loading. The reaction mixture was then left to stir overnight at room temperature. The mixture was transferred into a separatory funnel, followed by rinsing of the reaction vessel and stirrer with a total of 100 mL of dichloromethane giving a dichroic greenish-violet organic layer, which was washed once with 50 mL of 12% aqueous NH₄OH. After subsequently washing of the sample with brine (50 mL) and distilled water until neutral pH, the organic layer was concentrated on a rotary evaporator without using a drying agent (e.g., MgSO₄ or Na₂SO₄) to avoid losses by adsorption of aggregates. The greenish blue residue was taken up in dichloromethane and

added to the top of a chromatography column filled with silica gel ($H = 30$ cm, $\Phi = 2.5$ cm) which was eluted with a mixture of dichloromethane/*n*-hexane (80/20, v/v, degassed previously by sonication). A first eluted minor fraction of the zinc monocyano compound **6**, which is pink colored, was followed by the main fraction of the blue-green zinc dicyano compound **3**. By NMR, this fraction contains various amounts of the aromatic ligands which can be completely removed by resuspending the green residue (115 mg) in dry dichloromethane (2 mL) and inducing aggregation in 50 mL of dry *n*-heptane within a centrifuge vessel. Centrifugation for 5 min (Hettich centrifuge equipped with a 1624 rotor) at 3950 rpm for 5 min produced a slightly greenish supernatant, which was discarded, and a well-formed pellet. Resuspension in a fresh portion of *n*-heptane (20 mL) and centrifugation gave a colorless supernatant and a pellet which after drying in vacuum weighed 64.1 mg of pure **3** (68% yield). Upon doubling of the reaction scale, after boosting of the catalyst loading to 30 mol % and after the same workup procedure was followed, 107.1 mg of pure **3** could be obtained after centrifugation and drying (56% yield).

R_f (CH₂Cl₂ stabilized with amylenes) = 0.46. Mp: ~ 330 °C without decomposition. Compound **3** sublimates neatly with green vapors at 2.5×10^{-2} mbar. ¹H NMR (300 MHz, dioxane-*d*₆; δ , ppm): 9.90 (4H, d, $J = 4.8$, 3,7,13,17-H₄), 9.26 (4H, d, $J = 4.5$, 2,8,12,18-H₄), 8.24 (4H, d, $J = 1.5$, 2'-6'-H₂), 8.12 (2H, t, $J < 2$, 4'-H), 1.75 (s, 36H, *t*-Bu). In CDCl₃ broad signals due to aggregation are encountered. ¹³C NMR (75 MHz, dioxane-*d*₆; δ , ppm): 153.3, 152.2, 150.6, 135.8, 132.5, 131.2, 130.1, 129.6, 36.2 (CMe₃), 32.4 (CMe₃). Even after 40 000 scans the CN signal and the porphyrin quaternary carbons are not visible. UV-vis (CH₂Cl₂) [λ_{\max} , (log ϵ_{\max})]: 423 (5.56), 561 (4.06), 602 (4.55). FT-IR (KBr) [ν (cm⁻¹)]: 2962 (s), 2904 (m), 2869 (m), 2207 (vs), 1592 (m), 1536 (w), 1502 (w), 1420 (w), 1394 (w), 1362 (m), 1294 (mw), 1247 (mw), 1210 (m), 1077 (m), 1071 (m), 1004 (ms), 932 (ms), 902 (mw), 881 (m), 817 (m), 793 (vs), 716 (m), 709 (m). MS (MALDI-ToF) (m/z): 797.8, [M]⁺ with correct isotopic pattern; calcd for C₅₀H₅₀⁶⁴ZnN₆ = 798.4. HR-FAB-MS (m/z): 800.3540; calcd for C₅₀H₅₀⁶⁶ZnN₆ = 800.3357; calcd for [M + 2H]⁺ C₅₀H₅₂⁶⁴ZnN₆ = 800.3545.

5,15-Dicarboxy-10,20-bis(3,5-di-*tert*-butylphenyl)porphyrin (4). Porphyrin **3** (133 mg, 0.16 mmol) was stirred vigorously with 15 mL of H₂SO₄ (95–97%) and 3 drops water at 100 °C for 2 h and with exposure to air. The reaction was then cooled at room temperature and left to stir overnight. The solution was poured cautiously into ice–water. An attempt to extract the diacid with dichloromethane failed due to its low solubility. The green aqueous layer was neutralized with solid sodium dicarbonate, and then the aqueous solution was concentrated on rotary evaporation with caution. Intense foaming could be controlled by using a 250 mL flask and carefully controlling the bath temperature and vacuum level. The remaining solid was extracted with acetone in which the inorganic salts are insoluble. Final evaporation of the acetone extract left a raspberry colored powder (109 mg, 88% yield).

UV-vis (acetone) [λ_{\max} , (log ϵ_{\max})]: 411 (4.92), 508 (3.77), 584 (3.26). MS (MALDI-ToF) (m/z): 772.87. HR-FAB-MS (m/z): 772.3995; calcd for C₅₀H₅₂N₄O₄ [M – 2H]⁺ = 772.3989.

(5-Cyano-10,20-bis(3,5-di-*tert*-butylphenyl)porphyrinato)-zinc(II) (6). In a similar fashion, 5-bromo-10,20-bis(3,5-di-*tert*-butylphenyl)porphyrin free base (**5**)¹⁰ (100 mg, 0.13 mmol) was admixed with 35 mg of Pd₂(dba)₃ (0.04 mmol, 30 mol %), 43 mg of dppf (0.08 mmol, 60 mol %), 8 mg of activated Zn (90 mol %), 12 mg of Zn(CN)₂ (0.1 mmol, 80 mol %), and 12 mL

of anhydrous DMA. After stirring of the sample overnight at 120 °C and after workup as described above, isolation by column chromatography furnished 40 mg (40% yield) of pink-violet pure compound. Reproducible yields were obtained over several runs, but should the starting material have contained some dibromo compound (**2**) the final color of the reaction mixture was green.

R_f (CH_2Cl_2) = 0.64. ^1H NMR (300 MHz, CDCl_3 ; δ , ppm): 10.36 (1H, s, 15-H), 9.63 (2H, d, J = 4.8, 3,7- H_2), 9.41 (2H, d, J = 4.5, 13,17- H_2), 9.18 (2H, d, J = 4.5, 2,8- H_2), 9.10 (2H, d, J = 4.5, 12,18- H_2), 8.08 (d, 4H, J = 1.8, 2',6'- H_2), 7.85 (t, 2H, J = 1.8, 4'-H), 1.58 (s, 36H, *t*-Bu). ^{13}C NMR (75 MHz, 72 h, dioxane- d_8 ; δ , ppm): 152.8, 152.6, 151.7, 150.3, 142.8, 135.8, 133.8, 131.5, 131.2, 125.0, 123.5, 122.5, 86.3 (CN), 55.2 (impurity, CH_2Cl_2), 38.2, 36.2, 35.4, 32.5. UV-vis (CH_2Cl_2) [λ_{max} (log ϵ_{max}): 418 (5.57), 511 (3.50), 548 (4.19), 583 (4.02)]. MS (MALDI-ToF) (m/z): 774.04, $[\text{M}]^+$ with correct isotopic pattern. HR-FAB-MS (m/z): found, 775.3589; calcd for $\text{C}_{49}\text{H}_{53}\text{N}_5^{64}\text{Zn}$, 775.3592.

(5-Bromo-15-cyano-10,20-bis(3,5-di-*tert*-butylphenyl)porphyrinato)zinc (7**)**. 5-Cyano-10,20-bis(3,5-di-*tert*-butylphenyl)-porphyrinato zinc (**6**) (280 mg, 0.36 mmol) was dissolved in dichloromethane (150 mL), and the solution was cooled to 0 °C. Pyridine (1.0 mL) was added via a syringe. Then *N*-bromosuccinimide (96 mg, 0.54 mmol) was added in portions. The color of the reaction turns from pink to blue-violet. The reaction was stirred for 30 min at 0 °C and then quenched (after TLC control) with 15 mL of acetone. After the evaporation of the solvent, the violet-greenish residue was taken up in dichloromethane and deposited onto silica gel by vacuum evaporation. Column chromatography on silica gel (H = 20 cm, Φ = 6 cm) eluted with 98:2 dichloromethane/methanol (v/v) gave the main fraction of the green-violet compound **7** (215.5 mg, 70% yield).

R_f (CH_2Cl_2) = 0.61. ^1H NMR (300 MHz, dioxane- d_8 ; δ , ppm): 9.88 (d, 4H, J = 4.5), 9.77 (d, 4H, J = 4.5), 9.18 (d, 4H, J = 4.5), 9.05 (d, 4H, J = 4.5), 8.21 (s, 4H), 8.08 (s, 2H), 1.72 (s, 36H, $\text{C}(\text{CH}_3)_3$). ^{13}C NMR (75 MHz, dioxane- d_8 ; δ , ppm): 156.81, 153.47, 153.3, 152.05, 150.35, 150.25 (3',5'-C), 131.20 (2',6'-C), 126.17 (4'-C), 36.19 ($\text{C}(\text{CH}_3)_3$), 32.47 ($\text{C}(\text{CH}_3)_3$). UV-vis (CH_2Cl_2) [λ_{max} (log ϵ_{max}): 322 (4.11), 425 (5.44), 560 (4.03), 595 (3.92)]. FT-IR (KBr) [ν (cm^{-1}): 2957 (vs), 2907 (ms), 2863 (ms), 2202 (ms), 1592 (ms), 1555 (w), 1521 (w), 1521 (w), 1505 (w), 1477 (w), 1425 (w), 1393 (w), 1363 (ms), 1344 (w), 1322 (w), 1292 (w), 1246 (w), 1212 (w), 1074 (w), 1071 (w), 1059 (w), 1004 (ms), 950 (w), 937 (w), 898 (w), 882 (w), 816 (w), 807 (w), 793 (s), 766 (w), 737 (w), 729 (w), 715 (w), 698 (w), 668 (w)]. MS (MALDI-ToF) (m/z): 851.90; calcd for $\text{C}_{49}\text{H}_{50}\text{N}_5^{79}\text{Br}^{64}\text{Zn}$ $[\text{M}]^+$ = 851.25. HR-FAB-MS (m/z): 853.2528; calcd for $[\text{M}]^+$ $\text{C}_{49}\text{H}_{50}\text{N}_5^{81}\text{Br}^{64}\text{Zn}$ $[\text{M}]^+$ = 853.2521, $\text{C}_{49}\text{H}_{50}\text{N}_5^{79}\text{Br}^{66}\text{Zn}$ $[\text{M}]^+$ = 853.2510.

General Procedure for the Catalyst-Free Amination of meso-Bromoporphyrins. A solution of the above porphyrin **7** (50 mg) in excess amine (5 mL) was deaerated with nitrogen and then heated at 50 °C overnight. After evaporation of the amine, the residue was deposited onto silica gel by vacuum evaporation. Column chromatography on silica gel (H = 20 cm, Φ = 6 cm), eluted with dichloromethane, affords the title push-pull *N,N*-dialkylaminocyanoporphyrins (**8**).

(5-Morpholino-15-cyano-10,20-bis(3,5-di-*tert*-butylphenyl)porphyrinato)zinc (8a**)**. Using the above procedure, 50 mg of **7** (0.058 mmol) was heated overnight in 5 mL of morpholine at 50 °C. After chromatography, porphyrin **8a** was obtained as a blue-green powder (40 mg, 90% yield).

R_f (CH_2Cl_2) = 0.38. ^1H NMR (300 MHz, CDCl_3 ; δ , ppm): 9.59 (d, 2H, J = 4.5), 9.48 (d, 2H, J = 4.8), 8.96 (d, 2H, J = 4.8), 8.80 (d, 2H, J = 4.5), 7.98 (d, 4H, J = 1.8), 7.82 (d, 2H, J = 1.5), 3.99 (m, 4H, morpholinyl-H), 3.84 (m, 4H, morpholinyl-H), 1.56 (s, 36H, $\text{C}(\text{CH}_3)_3$). The chemical shifts are depending on the concentration. ^{13}C NMR (75 MHz, $\text{CDCl}_3/\text{dioxane-}d_8$, = 1/1, v/v; δ , ppm): 151.61, 150.29 (3',5'-C), 149.50, 148.34, 140.76, 134.79, 134.05, 131.20 (2',6'-C), 129.27, 129.00, 123.75, 120.67 (4'-C), 83.28 (CN), 68.11, 57.81, 34.42 ($\text{C}(\text{CH}_3)_3$), 31.01 ($\text{C}(\text{CH}_3)_3$). UV-vis (CH_2Cl_2) [λ_{max} (log ϵ_{max}): 316 (4.09), 424 (5.18), 557 (4.08), 592 (3.97)]. FT-IR (KBr) [ν (cm^{-1}): 3446 (b, residual water), 2957 (s), 2899 (ms), 2863 (ms), 2208 (ms), 1593 (m), 1552 (w), 1524 (w), 1501 (w), 1476 (w), 1444 (m), 1393 (w), 1348 (w), 1362 (ms), 1287 (w), 1260 (w), 1248 (w), 1213 (w), 1202 (w), 1172 (w), 1117 (w), 1095 (w), 1073 (w), 1059 (w), 971 (w), 930 (w), 915 (w), 900 (w), 882 (w), 861 (w), 820 (w), 798 (ms), 785 (ms), 729 (m), 715 (m)]. MS (MALDI-ToF) (m/z): 857.81; calcd for $\text{C}_{53}\text{H}_{59}\text{N}_6\text{O}^{64}\text{Zn}$ $[\text{M}]^+$ = 858.40. HR-FAB-MS (m/z): 859.4041; calcd for $\text{C}_{53}\text{H}_{59}\text{N}_6\text{O}^{64}\text{Zn}$ $[\text{M}]^+$ = 859.4042.

(5-Piperazino-15-cyano-10,20-bis(3,5-di-*tert*-butylphenyl)porphyrinato)zinc (8b**)**. In a flask equipped with a reflux condenser porphyrin, **7** (50 mg, 0.058 mmole) was stirred with a solution of 3.0 g of piperazine in 15 mL of chloroform. The general procedure was modified by adding a solvent because piperazine is a solid amine. The reaction mixture was heated at 50 °C under argon overnight. After the solvent was evaporated, the mixture of unreacted piperazine and the crude compound **8b** was extracted in the minimal quantity (ca. 10 mL) of dichloromethane. The column chromatography on silica gel (H = 20 cm, Φ = 6 cm) was eluted first with dichloromethane and afterward with a mixture of dichloromethane/methanol (95:5, v/v) to afford the porphyrin **8b** (25.8 mg, 52% yield).

R_f ($\text{CH}_2\text{Cl}_2/\text{MeOH}$, 90/10, v/v) = 0.60. ^1H NMR (300 MHz, dioxane- d_8 ; δ , ppm): 9.96 (broad s), 9.75 (broad s), 9.16 (broad s), 9.08 (broad s), 8.2 (broad s), 8.08 (broad s), 5.55 (broad s, *NH*-piperazinyl), 4.77 (broad s, 4H, piperazinyl-H), 4.05 (broad s, 4H, piperazinyl-H), 1.45 (s, 36H, $\text{C}(\text{CH}_3)_3$). UV-vis (CH_2Cl_2) [λ_{max} (log ϵ_{max}): 322 (3.84), 428 (4.6), 574 (3.89), 619 (3.88)]. FT-IR (KBr) [ν (cm^{-1}): 3295 (w), 2950 (s), 2935 (ms), 2849 (ms), 2207 (ms), 1592 (m), 1550 (w), 1444 (m), 1362 (ms), 1285 (m), 1247 (m), 1214 (m), 1069 (m), 1060 (m), 1001 (ms), 881 (w), 929 (w), 860 (w), 819 (m), 796 (s), 784 (m), 729 (w), 714 (w)]. MS (MALDI-ToF) (m/z): 856.86; calcd for $\text{C}_{53}\text{H}_{58}\text{N}_7^{64}\text{Zn}$ $[\text{M} - \text{H}]^+$ = 856.40. HR-FAB-MS (m/z): 858.4204; calcd for $\text{C}_{53}\text{H}_{60}\text{N}_7^{64}\text{Zn}$ $[\text{M} + \text{H}]^+$ = 858.4201.

(5-Piperidino-15-cyano-10,20-bis(3,5-di-*tert*-butylphenyl)porphyrinato)zinc (8c**)**. Following the general solventless procedure described above, compound **8c** was obtained as a blue-green powder (36.7 mg, 73% yield).

R_f (CH_2Cl_2) = 0.70. ^1H NMR (300 MHz, CDCl_3 ; δ , ppm): 9.58 (d, 2H, J = 4.5), 9.18 (d, 2H, J = 4.8), 8.95 (d, 2H, J = 4.8), 8.81 (d, 2H, J = 4.8), 8.02 (d, 4H, J < 2), 7.83 (t, 2H, J < 2), 4.33 (m, 4H, 2'',6''-piperidyl-H), 2.21 (m, 4H, 3'',5''-piperidyl-H), 2.09 (m, 2H, 4''-piperidyl-H), 1.55 (s, 36H, $\text{C}(\text{CH}_3)_3$). ^{13}C NMR (75 MHz, CDCl_3 ; δ , ppm): 152.37, 151.34, 150.61 (3', 5'-C), 149.71, 148.82, 140.92, 138.46, 134.79, 131.47, 130.02 (2', 6'-C), 129.52, 129.09, 124.62, 121.19 (4'-C), 82.92 (CN), 59.87, 35.05 ($\text{C}(\text{CH}_3)_3$), 31.73, 31.58 ($\text{C}(\text{CH}_3)_3$), 27.97, 25.03, 22.64, 14.12. See Supporting Information for H-C-correlated NMR spectra. UV-vis (CH_2Cl_2) [λ_{max} (log ϵ_{max}): 314 (4.18), 423 (5.22), 557 (4.06), 621 (3.95)]. FT-IR (KBr) [ν (cm^{-1}): 2949 (s), 2663 (w), 2210 (m), 1592 (m), 1554 (w), 1521 (w), 1442 (m), 1363 (m), 1283 (w), 1247 (m),

1213 (w), 1151 (w), 1118 (w), 1076 (w), 1001 (w), 930 (w), 915 (w), 881 (w), 865 (w), 825 (w), 791 (m), 729 (w), 714 (w). MS (MALDI-ToF) (m/z): 855.57; calcd for $C_{54}H_{59}N_6^{64}Zn$ [$M - H$] $^+$ = 855.41. HR-FAB-MS (m/z): 856.4168; calcd for $C_{54}H_{60}N_6^{64}Zn$ [M] $^+$ = 856.4171.

(5-Pyrrolidino-15-cyano-10,20-bis(3,5-di-*tert*-butylphenyl)porphyrinato)zinc (8d). Following the above solventless procedure, 50 mg of porphyrin **7** (0.058 mmol) heated in 5 mL of pyrrolidine affords after chromatography the porphyrin **8d** as a blue-green powder C (35.4 mg, 72% yield).

R_f (CH_2Cl_2) = 0.44. 1H NMR (300 MHz, dioxane- d_8 , at 30 °C; δ , ppm): 9.43 (d, 2H, J = 4.5), 9.35 (d, 2H, J = 4.2), 8.9 (d, 2H, J = 4.5), 8.66 (d, 2H, J = 4.5), 8.13 (d, 4H, J = 1.5), 8.01 (d, 2H, J < 2), 4.66 (t, 4H, pyrrolidinyl-H, J = 6.3), 2.60 (q, pyrrolidinyl-H, J < 2) 1.71 (s, 36H, $C(CH_3)_3$). ^{13}C NMR (75 MHz, dioxane- d_8 , at 30 °C; δ , ppm): 154.54, 150.43, 150.24, 150.19 (3',5'-C), 148.46, 142.95, 135.72, 130.705, 130.37 (2',6'-C), 129.24, 126.02, 122.25 (4'-C), 83.209 (CN), 61.23, 36.15 ($C(CH_3)_3$), 32.48 ($C(CH_3)_3$), 28.18. See Supporting Information for H-C-correlated NMR spectra. UV-vis (CH_2Cl_2) [λ_{max} (log ϵ_{max})]: 302 (4.18), 433 (5.23), 446 (5.07), 628.5 (4.27). FT-IR (KBr) [ν (cm^{-1})]: 2962 (s), 2870 (ms), 2197 (ms), 1592 (m), 1554 (m), 1521 (m), 1450 (ms), 1392 (w), 1362 (m), 1326 (m), 1247 (w), 1074 (w), 1006 (w), 880 (w), 826 (w), 789 (w), 728 (w). MS (MALDI-ToF) (m/z): 843.90; calcd for $C_{53}H_{59}N_6^{64}Zn$ [$M + H$] $^+$ = 843.41. HR-FAB-MS (m/z): 842.4019; calcd for $C_{53}H_{58}N_6^{64}Zn$ [M] $^+$ = 842.4014.

(5-*N,N*-Diethylamino-15-cyano-10,20-bis(3,5-di-*tert*-butylphenyl)porphyrinato)zinc (8e). The reaction was performed in a flask equipped with a reflux condenser under an argon-filled balloon. To the porphyrin **7** (50 mg, 0.058 mmol) was added 10 mL of diethylamine, and then the reaction mixture was heated overnight at 50 °C. After evaporation of the amine, column chromatography as described above afforded 39.6 mg of compound **8e** as a blue-green powder (81% yield).

R_f (CH_2Cl_2) = 0.90. 1H NMR (300 MHz, dioxane- d_8 , at 30 °C; δ , ppm): 9.69 (d, 4H, J = 2.7), 9.67 (d, 2H, J = 3), 9.09 (d, 2H, J = 4.8), 8.93 (d, 2H, J = 4.8), 8.21 (d, 4H, J = 1.8), 8.06 (d, 2H, J = 1.8), 4.55 (m, CH_2), 1.71 (s, 36H, $C(CH_3)_3$), 1.51 (t, CH_2 , J = 7.0). ^{13}C NMR (75 MHz, dioxane- d_8 , at 30 °C; δ , ppm): 153.35, 153.35, 151.68, 151.16, 150.36, 150.16 (3',5'-C), 142.98, 135.68, 132.58, 131.87, 130.90 (2',6'-C), 125.29, 123.50, 122.26 (4'-C), 85.11 (CN), 56.32, 36.18 ($C(CH_3)_3$), 32.49, 32.47 ($C(CH_3)_3$), 16.09. See Supporting Information for H-C-correlated NMR spectra. UV-vis (CH_2Cl_2) [λ_{max} (log ϵ_{max})]: 318 (4.15), 423 (5.30), 557 (4.07), 592 (3.95). FT-IR (KBr) [ν (cm^{-1})]: 2964 (s), 2892 (ms), 2871 (ms), 2210 (ms), 1591 (ms), 1552 (m), 1522 (w), 1501 (w), 1443 (m), 1392 (w), 1362 (ms), 1283 (m), 1283 (m), 1221 (m), 1119 (w), 1070 (m), 1002 (m), 929 (w), 899 (w), 881 (w), 824 (m), 792 (ms), 765 (w), 728 (m), 713 (ms). MS (MALDI-ToF) (m/z): 845.87; calcd for $C_{53}H_{61}N_6^{64}Zn$ [$M + H$] $^+$ = 845.42. HR-FAB-MS (m/z): 844.4178; calcd for $C_{53}H_{60}N_6^{64}Zn$ [M] $^+$ = 844.4171.

5,15-Dimorpholino-10,20-bis(3,5-di-*tert*-butylphenyl)porphyrin (9). 5,15-Dibromo-10,20-bis(3,5-di-*tert*-butylphenyl)porphyrin (**2**, 50 mg, 0.06 mmol) was dissolved in 5 mL of morpholine, the solution was stirred for 72 h at 50 °C. Column chromatography on silica gel (H = 20 cm, Φ = 6 cm) after elution first with dichloromethane which afforded a minor fraction of 5-bromo-15-morpholino-10,20-bis(3,5-di-*tert*-butylphenyl)porphyrin (8.6 mg) and then with dichloromethane/methanol = 90/10 (v/v) provided the compound **9** which was obtained as a cognac colored powder (25 mg, 49% yield).

R_f (CH_2Cl_2) = 0.88. 1H NMR (300 MHz, $CDCl_3$, at 30 °C; δ , ppm): 9.58 (d, 4H, J = 4.5), 8.85 (d, 4H, J = 4.8), 8.067 (s, 4H), 7.84 (d, 2H, J = 1.2), 4.37 (m, 8H, morpholinyl-H), 4.30 (m, 8H, morpholinyl-H), 1.56 (s, 36H, $C(CH_3)_3$), -2.68 (s, 2H, NH). ^{13}C NMR (75 MHz, $CDCl_3$, at 30 °C; δ , ppm): 148.79 (3',5'-C), 141.17 (1'-C), 129.68 (2',6'-C), 129.03, 123.99, 121.65 (4'-C), 121.03, 69.04, 57.75, 35.07 ($C(CH_3)_3$), 31.71 ($C(CH_3)_3$). UV-vis (CH_2Cl_2) [λ_{max} (log ϵ_{max})]: 304 (4.13), 422 (5.35), 519 (4.05), 558 (3.85), 657 (3.53). FT-IR (KBr) [ν (cm^{-1})]: 3446 (b), 3317 (m), 3960 (s), 2899 (ms), 2848 (ms), 1591 (m), 1505 (w), 1473 (m), 1446 (m), 1392 (w), 1363 (m), 1301 (w), 1262 (m), 1244 (m), 1196 (w), 1172 (w), 1151 (w), 1113 (s), 1066 (w), 1033 (m), 976 (w), 946 (w), 915 (w), 898 (w), 880 (w), 794 (s), 729 (m), 715 (m). MS (MALDI-ToF) (m/z): 857.09; calcd for $C_{56}H_{69}N_6O_2$ [$M + H$] $^+$ = 857.54. HR-FAB-MS (m/z): 857.5479; calcd for $C_{56}H_{69}N_6O_2$ [$M + H$] $^+$ = 857.5482.

5-Morpholino-10,20-bis(3,5-di-*tert*-butylphenyl)porphyrin (10). Similar to the general procedure, 5-bromo-10,20-bis(3,5-di-*tert*-butylphenyl)porphyrin (**5**, 50 mg, 0.065 mmol) was heated in 5 mL of morpholine. Column chromatography afforded the main product **10** as a red powder (31 mg, 61% yield).

R_f (CH_2Cl_2) = 0.79. 1H NMR (300 MHz, $CDCl_3$; δ , ppm): 10.11 (s), 9.73 (d, 2H, J = 4.8), 9.28 (d, 2H, J = 4.8), 9.025 (d, 2H, J = 4.5), 8.99 (d, 2H, J = 4.8), 8.12 (d, 4H, J = 1.8), 7.85 (d, 2H, J = 1.8), 4.40 (dm, 8H, morpholinyl-H), 1.56 (s, 36H, $C(CH_3)_3$), -2.90 (s, 2H, NH). ^{13}C NMR (75 MHz, $CDCl_3$; δ , ppm): 148.90 (3',5'-C), 140.72 (1'-C), 131.69, 130.88, 129.97, 129.67 (2',6'-C), 128.59, 121.07 (4'-C), 120.20, 57.83, 35.07 ($C(CH_3)_3$), 31.76 ($C(CH_3)_3$). See Supporting Information for H-C-correlated NMR spectra. UV-vis (CH_2Cl_2) [λ_{max} (log ϵ_{max})]: 302 (4.08), 415 (5.41), 511 (4.11), 547 (3.73), 584 (3.65), 642 (3.65). FT-IR (KBr) [ν (cm^{-1})]: 3313 (b), 2989 (s), 2899 (ms), 2856 (ms), 1591 (ms), 1474 (m), 1392 (w), 1362 (ms), 1298 (w), 1263 (m), 1245 (ms), 1153 (w), 1115 (m), 1063 (w), 1032 (w), 984 (w), 963 (m), 916 (m), 898 (w), 879 (w), 842 (w), 816 (w), 794 (ms), 716 (m), 690 (w). MS (MALDI-ToF) (m/z): 771.86; calcd for $C_{52}H_{61}N_5O$ [M] $^+$ = 771.49. HR-FAB-MS (m/z): 772.4961; calcd for $C_{52}H_{62}N_5O$ [$M + H$] $^+$ = 772.4954.

5-Morpholino-15-cyano-10,20-bis(3,5-di-*tert*-butylphenyl)porphyrin Free Base (11a). Porphyrin **8a** (15 mg, 0.017 mmole) was stirred with a mixture of deoxygenated trifluoroacetic acid (3 mL), sulfuric acid (3 mL), and 3 drops distilled water for 2 h at room temperature. The reaction mixture was poured very slowly and carefully on crushed ice (20 g) under stirring. The resulting mixture was extracted with dichloromethane (2 \times 20 mL), washed with sodium carbonate (2 \times 30 mL), and then with distilled water until neutral pH. After evaporation of the solvent, the violet residue was taken up in dichloromethane and deposited onto silica gel by vacuum evaporation. After column chromatography on silica gel (H = 15 cm, Φ = 2 cm), eluted with dichloromethane/methanol = 98/2, v/v, the violet free base porphyrin was obtained in 97% yield (13.4 mg).

R_f (CH_2Cl_2) = 0.58. 1H NMR (300 MHz, $CDCl_3$; δ , ppm): 9.47 (d, 2H, J = 4.8), 9.42 (d, 2H, J = 4.8), 8.92 (d, 2H, J = 4.8), 8.71 (d, 2H, J = 4.8), 8.01 (d, 4H, J = 1.5), 7.84 (d, 2H, J = 1.5), 4.39 (s, 4H, morpholinyl-H), 4.38 (s, 4H, morpholinyl-H), 1.55 (s, 36H, $C(CH_3)_3$), -1.90 (s, 2H, NH). ^{13}C NMR (75 MHz, $CDCl_3$; δ , ppm): 149.20 (3',5'-C), 139.97 (1'-C), 135.35, 129.68 (2',6'-C), 123.99, 121.65 (4'-C), 96.47, 83.14 (CN), 68.79, 58.43, 35.07 ($C(CH_3)_3$), 31.71 ($C(CH_3)_3$). UV-vis (CH_2Cl_2) [λ_{max} (log ϵ_{max})]: 426 (5.26), 524 (3.97), 561 (3.91),

561 (4.02), 651 (3.61). FT-IR (KBr) [ν (cm^{-1})]: 3460 (b, residual water), 3309 (ms), 2961 (s), 2906 (ms), 2663 (ms), 2213 (m), 1593 (m), 1480 (w), 1363 (m), 1248 (m), 865 (w), 796 (ms), 716 (m). MS (MALDI-ToF) (m/z): 797.02; calcd for $\text{C}_{53}\text{H}_{61}\text{N}_6\text{O}$ [$M + \text{H}$] $^+$ = 797.49. HR-FAB-MS (m/z): 797.4915; calcd for $\text{C}_{53}\text{H}_{61}\text{N}_6\text{O}$ [$M + \text{H}$] $^+$ = 797.4906.

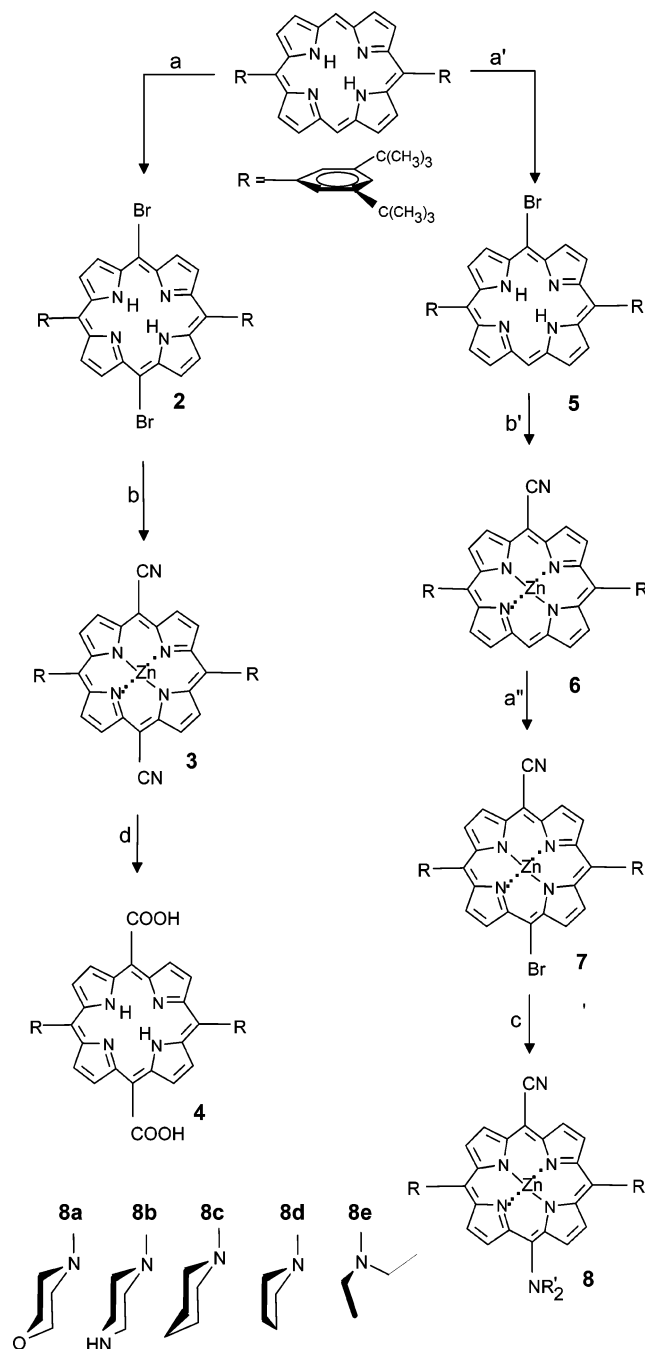
Time-Resolved Fluorescence. For the time-resolved fluorescence measurements, we used a Ti:sapphire laser delivering sub-150 fs pulses at a repetition rate of 76 MHz. To excite the compound to second harmonic generation, we employed a BBO crystal. Predominantly one species only could be excited, either the monomers or the aggregates, by tuning the excitation wavelength to 419 and 447 nm, respectively. The spectral width of the pulses was about 5 nm so that excitation conditions are comparable to that of the stationary measurements. A closed loop circulation system consisting of an optics cuvette and a peristaltic pump avoided photodegradation of the compounds. The fluorescence signal was detected by a streak camera (Hamamatsu C5680) coupled to a spectrometer (Jobin-Yvon HR460, 100 lines/mm grating). Fluorescence spectra were measured in the wavelength range between 580 and 755 nm, with a spectral resolution of 2 nm and a temporal resolution of 8 ps. A polarizer was used for compensating the effect of molecular rotation on the fluorescence decay. The obtained fluorescence spectra were analyzed globally in terms of decay-associated emission spectra (DAES) by fitting the following function to the data:

$$I(\lambda, t) = \sum_{i=1}^n A_i(\lambda) e^{-t/\tau_i}$$

Here $I(\lambda, t)$ is the fluorescence intensity, $A_i(\lambda)$ are the spectral weights, and τ_i are the global decay times.

Crystallographic Details. The data collection of $3 \cdot 2\text{CHCl}_3$ was carried out at the ANKA synchrotron source (Forschungszentrum Karlsruhe) on a Bruker AXS D8 diffractometer equipped with a SMART APEX CCD ($\lambda = 1.0 \text{ \AA}$) while $3 \cdot 2\text{C}_4\text{D}_8\text{O}_2$ was measured on a STOE IPDS (image plate diffraction system) with $\lambda = 0.8 \text{ \AA}$ at 150 K. The structure solutions and full-matrix least-square refinements based on F^2 were performed with SHELX-97 program package.¹¹ Molecular diagrams were prepared using the program Diamond.¹² $3 \cdot 2\text{CHCl}_3$: dark green needles, $0.1 \times 0.04 \times 0.04 \text{ mm}$; $M_r = 1039.1$; monoclinic, space group $P2_1/n$ (No. 14); $a = 6.060(4)$, $b = 17.733(10)$, $c = 23.562(13) \text{ \AA}$; $\beta = 96.869(13)^\circ$; $V = 2514(3) \text{ \AA}^3$; $Z = 2$; $D_c = 1.373 \text{ g cm}^{-3}$; $\mu(\lambda = 1 \text{ \AA}) = 2.219 \text{ mm}^{-1}$ giving a final R1 value of 0.0788 for 356 parameters and 2878 unique reflections with $I \geq 2\sigma(I)$ and wR2 of 0.2272 for all 8836 reflections ($R_{\text{int}} = 0.1692$). A disorder has been modeled for two symmetry-equivalent *tert*-butyl groups (C17–C20). However most of the residual peaks namely Q1–Q6 with a maximum of 1.007 e/\AA^3 are still located in this area but could not be refined in a suitable model. $3 \cdot 2\text{C}_4\text{D}_8\text{O}_2$: violet plates, $0.26 \times 0.12 \times 0.04 \text{ mm}$; $M_r = 1064.6$; triclinic, space group $P\bar{1}$ (No. 2); $a = 7.6081(15)$, $b = 10.239(2)$, $c = 19.051(4) \text{ \AA}$; $\alpha = 77.14(3)$, $\beta = 88.95(3)$, $\gamma = 72.70(3)^\circ$; $V = 1379.6(5) \text{ \AA}^3$; $Z = 1$; $D_c = 1.311 \text{ g cm}^{-3}$; $\mu(\lambda = 1 \text{ \AA}) = 0.703 \text{ mm}^{-1}$ giving a final R1 value of 0.0572 for 488 parameters and 3245 unique reflections with $I \geq 2\sigma(I)$ and wR2 of 0.1510 for all 6848 reflections ($R_{\text{int}} = 0.1079$). CCDC-632909 and CCDC-653012 contain the supplementary crystallographic data for this paper. These data can be obtained free of charge at www.ccdc.cam.ac.uk/conts/retrieving.html [or from the Cambridge Crystal-

SCHEME 1: Reagents and Reaction Conditions: (a) NBS, Pyridine, CH_2Cl_2 , RT, 30 min 74%; (a') NBS, Pyridine, CHCl_3 , 0°C , 10 min 70%; (a'') NBS, Pyridine, CH_2Cl_2 , 0°C , 30 min 70%; (b) $\text{Zn}(\text{CN})_2$, Zn, $\text{Pd}_2(\text{dba})_3$, DPPF, DMA, 120°C , 4 h. 68%; (b') $\text{Zn}(\text{CN})_2$, Zn, $\text{Pd}_2(\text{dba})_3$, DPPF, DMA, 120°C , 12 h. 40%; (c) Alk_2NH Excess, 50°C , 18 h, 49–90%. (d) TFA, H_2SO_4 , H_2O , 100°C , 2 h, 88%

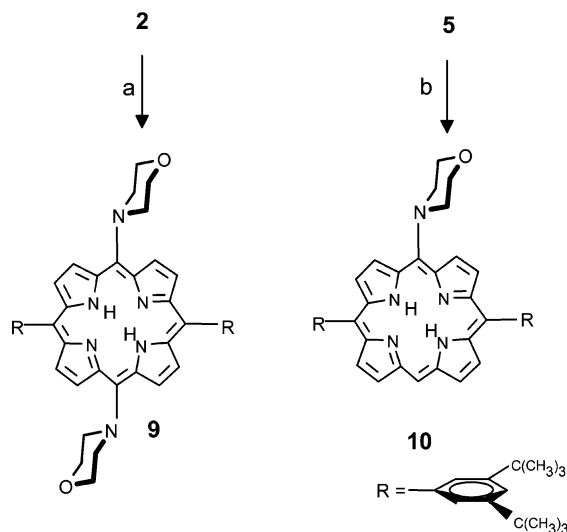


lographic Data Centre, 12 Union Road, Cambridge CB2 1EZ, U.K.; fax, (internat.) +44-1223/336-033; e-mail, deposit@ccdc.cam.ac.uk].

Results and Discussion

Syntheses. By discovering that hydrogen bonding is not a prerequisite for inducing chlorosomal-type organization of pigments, we could generalize this self-assembly algorithm.¹³ Reasoning that π – π interactions combined with weak electrostatic and dispersive forces can also be engineered with other

SCHEME 2: Both Reactions Carried Out in Excess Morpholine at 50 °C: (a) 72 h, Isolated Yield = 49%; (b) 12 h, Isolated Yield = 61%



recognition groups than the ones present in BChls (i.e., as in the Zn porphyrin **1**), we synthesized the title compound **3** in over 65% yield by a palladium-catalyzed cyanation (see Scheme 1) starting from the known 5,15-dibromo-10,20-bis(3,5-di-*tert*-butylphenyl)porphyrin (**2**)¹⁰ and zinc cyanide.^{14a} The mono-5-cyanoporphyrin **6** was obtained as a byproduct (10% yield), and it could be prepared in an independent way by the same coupling procedure^{14a} from the corresponding 5-bromoporphyrin **5** obtained by the method of Arnold.¹⁵ While this work was in progress, other direct cyanations of bromoporphyrins^{14b} and haloindoles^{14c} have been reported with similar yields. This reaction has an induction phase which depends on the catalyst loading and on the concentration of the zinc cyanide. For larger scale reactions, as an excess of cyanide ions poisons the catalyst,¹⁶ we recommend addition of a fresh portion of catalyst after 90 min and when complete metalation of the free base porphyrin has occurred. It has been reported for other cyanation reactions that water can act as a cocatalyst;¹⁷ however, in the present case, moisture as well as oxygen inhibit the reaction.

With the monocyanoporphyrin **6** in hand we could optimize a catalyst-free, solventless amination of the novel 5-cyano-15-bromo zinc porphyrin **7**. We were inspired by the recent amination of brominated perylene diimides discovered by Imahori and co-workers.¹⁸ The high yields and facile workup recommend this reaction for obtaining push–pull porphyrins having the donor ($\text{D} = \text{NR}_2$) and acceptor ($\text{A} = \text{CN}$) groups directly linked to the *meso* positions. There are ample examples of porphyrins where the D/A groups are linked via phenyl or ethynyl spacer groups onto the porphyrin macrocycle.¹⁹ The herein described procedure affords for the first time such push–pull porphyrins with direct, linkerless attachment of the D/A groups. An analogy to 4-*N,N*-dialkylaminobenzonitriles, dual fluorescent and well-studied compounds, both experimentally and theoretically,²⁰ is obvious. Previously synthesized *meso-N,N*-dialkylaminoporphyrins employed either Pd-catalyzed Buchwald–Hartwig conditions²¹ or required the presence of Ni(II) salts.²² The direct amination of *meso*-bromoporphyrins works well also for the compounds **2** and **5** yielding the free bases **9** and **10**, respectively (Scheme 2), but from the former reaction it was not possible to isolate the intermediate 5-(dialkylamino)-15-bromoporphyrin as this reacts more rapidly to the 5,15-bis-(dialkylamino)porphyrin (**9**). For obtaining *meso*-substituted push–pull porphyrins, the sequence monobromination, cyana-

tion, bromination, and amination gives higher yields than the alternate one involving bromination of the 5-(dialkylamino)-porphyrin. Probably protonation occurs so that the NBS bromination of the 5-dialkylammonium salt is much slower than the *meso*-bromination of the 5-cyanoporphyrin. We could thus prove that even *meso*-brominated free base porphyrins can be successfully aminated. The presence of nickel salts as catalysts, as recently stated,²² is not needed in this direct and facile reaction.

Photophysical Properties. An interesting feature of the title compound **3** is it is aggregate-induced emission.²³ Figure 1 shows the absorption and in the inset the fluorescence spectrum of **3** as a mull in perfluoropolyalkyl ether oil. Usually, with randomly oriented chromophores self-quenching or concentration quenching prevent observing steady-state fluorescence from strongly absorbing solids. Due to the very orderly manner in which the chromophores **3** are arranged (vide infra), after excitation at 430–500 nm a weak but measurable emission is observed. The fluorescence excitation spectra monitored at a wavelength where only the aggregates emit (700 nm) show that the Soret band is severely broadened, in contrast to the sharp band encountered for the monomers (at 413 nm) when the excitation was monitored at 645 nm (Figure 1).

Time-resolved measurements followed by fitting of the decay-associated emission spectra (DAES) reveal two components which can be assigned to the monomers and to the aggregates by excitation at 419 nm (Figure 2). When exciting at 447 nm, where the monomers do not absorb, the longer-lived, monomer fluorescence is absent, the spectrum equals the DAES, and the fitting algorithm finds only one (1.2 ns) component (Figure 2). Thus, the fluorescence is relatively strongly, but not entirely, quenched in the aggregates and the lifetime is somewhat shortened. However, a 1 ns lifetime is exceptionally long for aggregated chromophores and should allow efficient trapping of the radiant energy. The unquenched fluorescence and therefore long lifetime is a strong indication of a very orderly manner in which the porphyrins are arranged. With unspecific aggregation, fluorescence in the solid state is usually very strongly quenched and the lifetimes are in the ps to sub-ps time range. These optical properties are typical of natural self-organized antenna systems, like the chlorosomes, and make aggregates of **3** a promising candidate for light-harvesting in artificial devices. We reported recently very similar absorption and fluorescence properties for an isomer of the BChl *c* mimic **1** having the (*rac*)-hydroxyethyl group in the 3-position and the acetyl group in the 13-position of the macrocycle.²⁴

The push–pull zinc porphyrins **8a,b** self-assemble similarly to **3** in thoroughly dried nonpolar solvents (Figure 3). In contrast **8c–e** do not show any evidence of self-association in the same solvents.

It is evident from the above spectra that a similar self-assembly algorithm must operate for the dicyanozinc porphyrin **3** and the push–pull Zn–morpholino–cyano compound **8a**. However, in the latter, self-assembly could additionally occur via coordination of the zinc atom by the morpholinyl oxygen from one side of the macrocycle combined with a cyano–zinc interaction on the other side. The piperazino-substituted compound **8b** also self-assembles but gives a split and less broadened Soret band (Figure 4). In control experiments performed with the same solvents, the piperidino (**8c**), pyrrolidino (**8d**), and diethylamino (**8e**) analogs did not give self-assemblies as judged by the nonscattering solutions in *n*-heptane and by the monomeric type of absorption and fluorescence spectra (Figure 4 and see also Supporting Information).

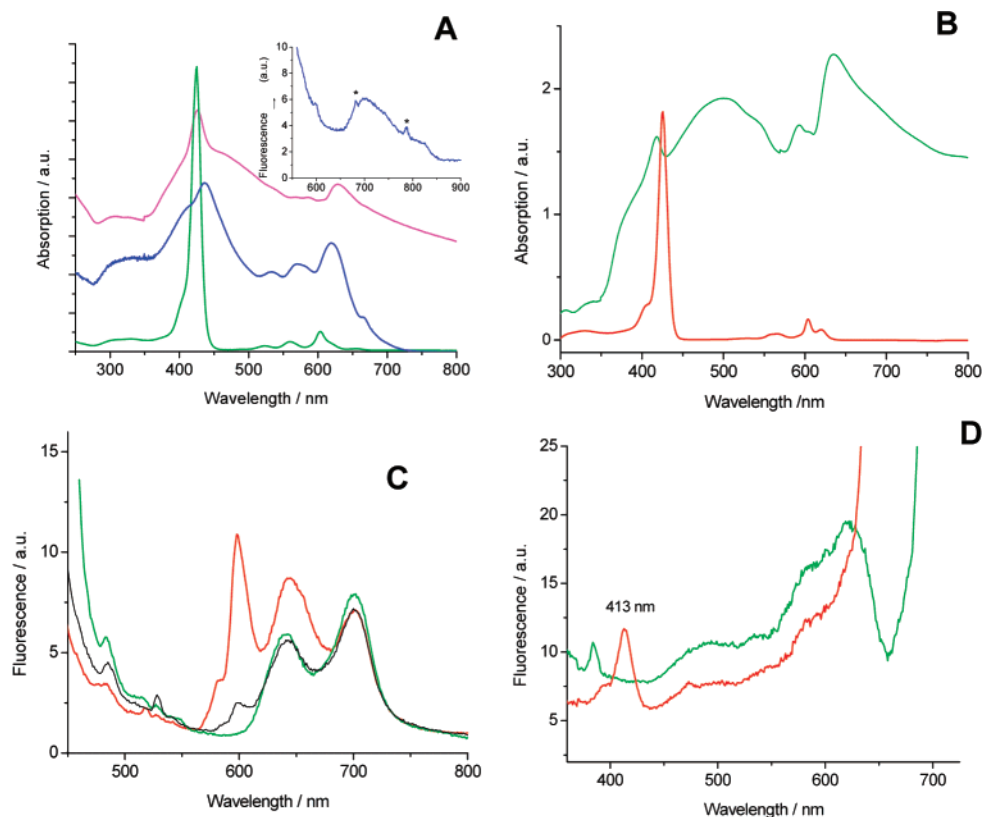


Figure 1. (A) Absorption spectra of **3**. Blue trace: crystals rubbed between two quartz plates with perfluoropolyalkyl ether oil (ABCR, Karlsruhe, Germany), which were measured in an integrating sphere on a Cary 500 UV–vis–NIR spectrometer. Inset: fluorescence measured on a Cary Eclipse fluorimeter at right angle from a similar sample with 500 nm excitation. The asterisks denote spikes which do not come from the sample. Magenta trace: same sample but measured as normal absorption after addition of one drop of dry dichloromethane. Green trace: same sample after dissolution in dichloromethane, path length 1 mm. (B) Green trace: absorption spectrum of **3** suspended in *n*-heptane after short sonication with a path length of 1 cm. The baseline is shifted due to strong scattering from the aggregates. Red trace: after addition of one drop of methanol the aggregates are disrupted and the monomeric **3**•MeOH adduct is formed, path length 1 mm. (C) Stationary fluorescence spectra of aggregates suspended in *n*-heptane with different excitation wavelengths: red trace, 420 nm excitation; black trace, 430 nm excitation; green trace, 450 nm excitation. (D) Fluorescence excitation spectra monitored at 700 (green trace) and 645 nm (red trace).

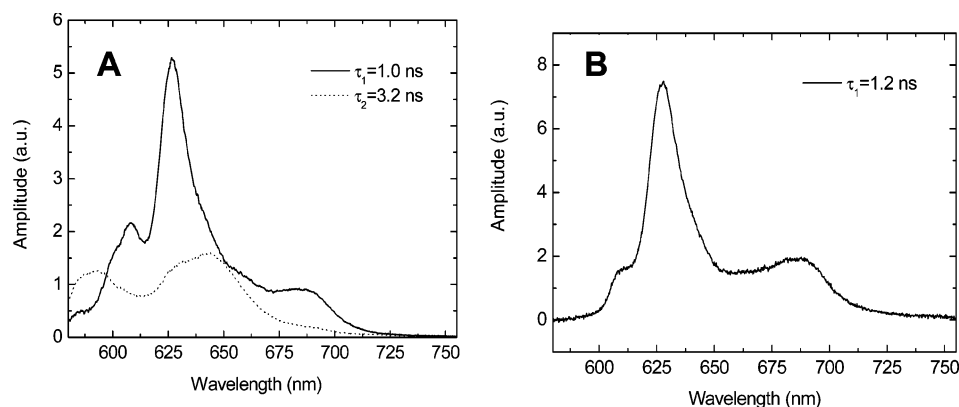


Figure 2. DAES from aggregates of **3** in dry *n*-heptane. Excitation wavelength was 419 nm (A, at left) and 447 nm (B, at right). For color-coded images of the fluorescence and the goodness of fit, see the Supporting Information.

Energy transfer between the singlet excited-state of zinc porphyrins and their free bases is well documented both in covalent²⁵ and hydrogen-bonded constructs.²⁶ We have investigated by time-resolved fluorescence mixtures in *n*-heptane of the zinc porphyrin **8a** with 5% and 10% addition of its corresponding free base **11a**. Although the aggregate and free base fluorescence were clearly evident with lifetimes of ~ 1.0 and 7.0 ns, respectively, we could not distinguish in the DAES an energy transfer component (data not shown). This indicates that the self-assembly of the zinc porphyrins occurs without intermixing of their free bases which must thus be separated by a distance larger than the Förster radius.^{26f}

Single-Crystal X-ray Diffraction Structures. Needlelike crystals (inset in Figure 5) could be grown reproducibly either by slow evaporation of CDCl_3 from a capped 5 mm diameter NMR tube or by slowly diffusing cyclohexane into a concentrated chloroform solution of **3** through an intermediate layer of a cyclohexane–chloroform mixture. Because these microcrystals diffracted only weakly X-rays, synchrotron radiation had to be used to obtain data sets which finally led to solving the crystal structure by direct methods.¹¹ The molecular structure is shown in Figure 5A and shows the expected geometry. Figure 5B shows that the tetrapyrroles stack as a flight of stairs with a slightly off-set geometry, as expected from the strong π – π

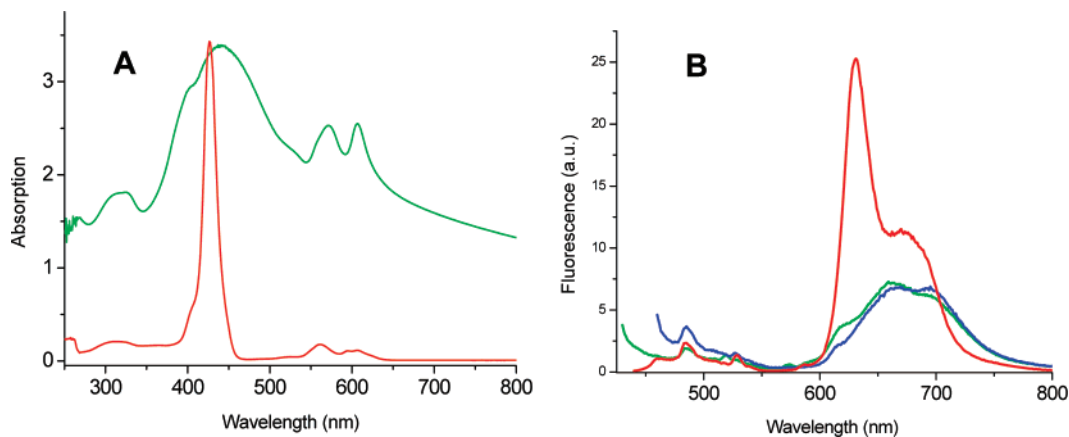


Figure 3. (A) Absorption spectra of **8a** in *n*-heptane (green trace) and after addition of a methanol aliquot and 3-fold dilution with *n*-heptane. A few drops of dichloromethane were added to ensure a homogeneous solution (red trace). (B) Corresponding stationary fluorescence spectra of the aggregated species with excitation at 420 (green trace) and 450 nm (blue trace) and of the Zn-methanol adduct excited at 430 nm (red trace).

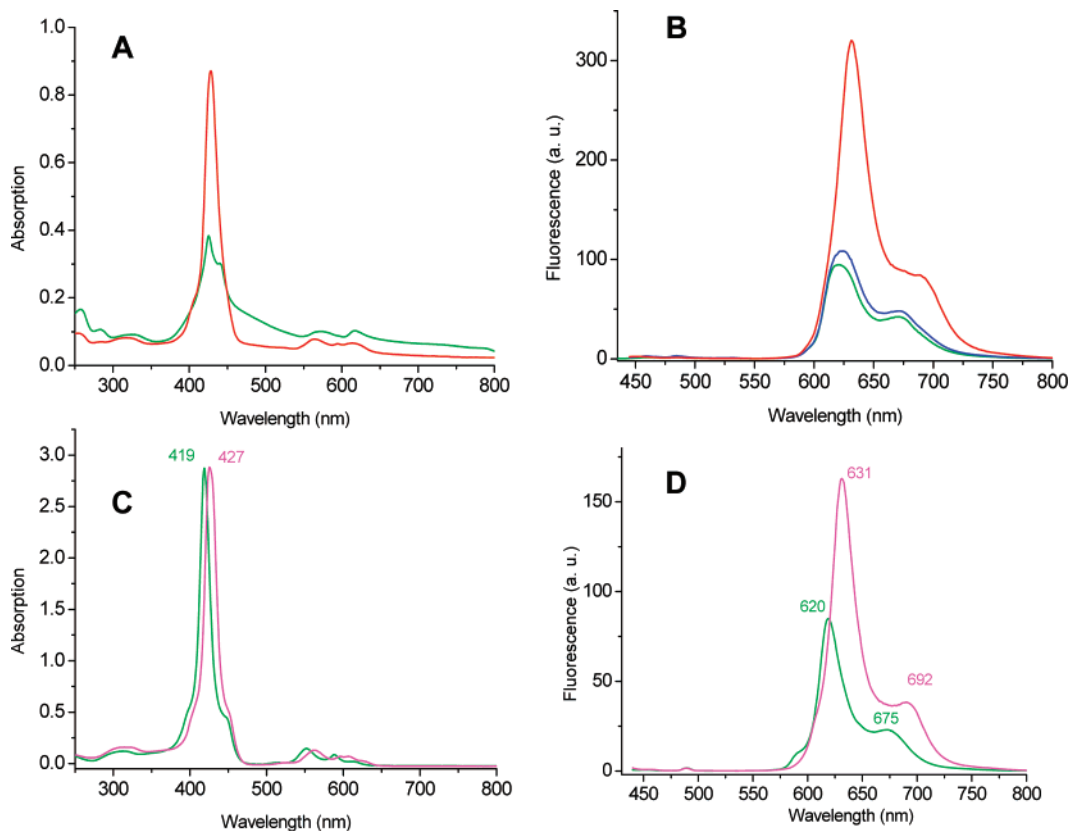


Figure 4. Comparison of the absorption (A, C) and fluorescence spectra (B, D) of **8b** (A, B) and **8e** (C, D). (A) Absorption spectra of **8b** after sonication in *n*-heptane (green trace) and after addition of an aliquot of methanol and 2-fold dilution with *n*-heptane (red trace). Note the split and broadened Soret band. (B) Corresponding fluorescence of **8b** in *n*-heptane (green trace, excitation wavelength at 425 nm; blue trace, excitation wavelength at 435 nm) and after addition of methanol (red trace, excitation wavelength at 433 nm). (C) Absorption spectra of **8e** in *n*-heptane (green trace) and after addition of an aliquot of methanol (magenta trace). (D) Corresponding fluorescence spectra of **8e** in *n*-heptane (green trace, excitation wavelength at 420 nm) and after addition of an aliquot of methanol (magenta trace excitation wavelength at 430 nm).

interaction between electron deficient porphyrins.²⁷ Figure 5C represents the packing of stacks along the short crystallographic axis. Well-ordered chloroform solvent molecules are included in the crystal lattice, and a C–D(H)–N–C interaction with the C–N distance of 3.17 Å is encountered. There are no short contacts between the stacks which define a rhombus with 14.67 and 16.47 Å Zn–Zn spacings. Within a stack Zn–Zn distances are 6.011 Å.

The stacking interaction with a 3.399 Å spacing between the porphyrin planes is interesting as a similar stacking was encountered in the natural BCHs as put into evidence with solid state ¹³C NMR on uniformly ¹³C-labeled BCHl^{5a,28} and in the

two crystal modifications of **1**.⁹ The dotted lines in Figure 4B (3.111 Å long) are only a guide to the eye and should not be interpreted as “bonds” but as a newly put into evidence electrostatic interaction between the electron-deficient zinc atom and the electron-rich nitrogens within the pseudohalogen groups. The strongly interacting chromophores lead to a considerable broadening of the Soret and Q bands as shown in Figures 1 and 2, and the aggregate maxima are red-shifted as in J-aggregates. Usually J-aggregates have sharp absorption maxima.²⁹ In our case the inhomogeneous broadening of the absorption can be assigned to size heterogeneity in the length of the stacks. For light-harvesting purposes this is quite beneficial as the whole

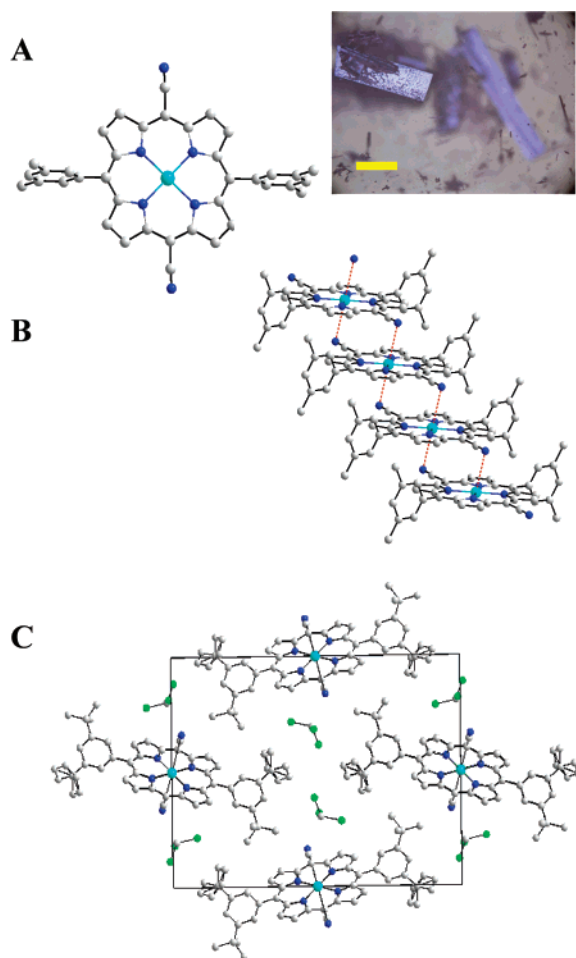


Figure 5. Crystal structure and packing of **3**. (A) Monomeric unit. Inset: microcrystals under the light microscope. The yellow scale bar is 50 μm long. (B) Stacks formed by π - π stacking and a CN-Zn electrostatic interaction (dotted red line 3.111 Å). (C) View of stacks along the short crystallographic *a*-axis showing inclusion of chloroform as well-ordered crystallization solvent. A weak $\text{Cl}_3\text{C-H-N}\equiv\text{C}$ interaction is encountered. One of the *tert*-butyl groups in each 3,5-di-*tert*-butylphenyl substituents is disordered over two preferential positions. In (A) and (B) the *tert*-butyl groups have been replaced by the *ipso*-carbon atom for clarity. Color coding: C, gray; N, blue; Zn, cyan; Cl, green. H atoms have been omitted for clarity.

spectral range up to over 700 nm is covered. In dichloromethane the self-assemblies completely dissociate and only a monomeric-type spectrum is obtained (green trace in Figure 1A). This implies that the CN-Zn electrostatic interaction at low concentrations does not survive a solvent of even medium polarity. In more concentrated CDCl_3 solutions aggregation shifts are encountered in the ^1H NMR spectra (data not shown).

It is remarkable that the combination of π -stacking with this for the first time visualized electrostatic interaction wins over a putative direct coordination of the zinc atom by the nitrogen lone pair. Self-assembly into stacks is thermodynamically driven, and the packing of stacks involves multiple hydrophobic interactions.

From dioxane a different crystal packing is encountered which includes two solvent molecules/unit cell. While one spectator dioxane molecule has just a space filling role, a second one is ligating the zinc atoms in two stacked porphyrins with an interplanar distance of 7.115 Å (Figure 6). The Zn-O ligations are 2.596 Å long and much stronger than the previously described Zn-N \equiv C interactions. Due to the intercalated diox-

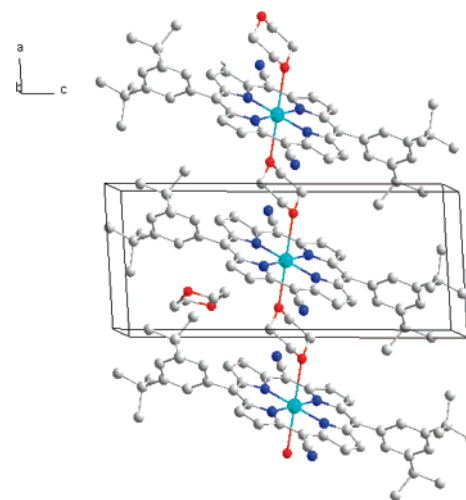


Figure 6. Cocystal of **3** with dioxane. The stacks pack solely by hydrophobic interactions. Zn-Zn spacings within a stack are 7.608 Å, while the closest Zn-Zn spacing within adjacent stacks is 10.239 Å.

anes, a much more loosely stacked structure with partial loss of the π - π interactions is encountered. The Zn-Zn spacings within a stack are 7.608 Å, only slightly longer than those in Figure 5 due to a larger overlap of the porphyrin rings. Both crystal structures have in common the hydrophobic packing of stacks. Presently it is difficult to predict a priori the outcome of crystallization when multiple weak interactions act in conjunction.³⁰ Modeling of polymorphs is an active research area, and the present structures may serve as an example where the π - π stacking combined with weak electrostatic interactions can be outmaneuvered by a more strongly bis-coordinating solvent, like dioxane.

Conclusions

The crystal structures of **3** prove that the structural constraints to obtain a chlorosomal type self-assembly can be relaxed and that other functional groups than the ones encountered in BChl-(s) (i.e., 1-hydroxyethyl, carbonyl, and a central metal atom) can be used. Shorter and high yielding synthetic routes can then furnish functional light-harvesting assemblies.¹³ The advantage of our compounds is that they are fully synthetic and culturing of bacteria or isolation of Chl *a* from algae can be avoided. Our strategy, which starts from preformed porphyrins and then uses substitution reactions, is optimal if larger quantities of material are desired. The mono- and dicyano compounds described herein are interesting building blocks amenable to further chemistries as for example they can be easily hydrolyzed to the corresponding carboxylic acids (e.g., **4**). The push-pull dialkylamino-cyano-porphyrins could be used in field-effect transistors or may have interesting second order nonlinear harmonic generation properties which are currently under investigation. Progress along these lines of research will be reported in due course.

Acknowledgment. This work was partially supported by the DFG Center for Functional Nanostructures at the University of Karlsruhe through Project C3.5 (T.S.B. and H.K.).

Supporting Information Available: Additional spectroscopic data (24 figures). This material is available free of charge via the Internet at <http://pubs.acs.org>.

References and Notes

- (1) (a) Frigaard, N. U.; Bryant, D. A. Complex Intracellular Structures in Prokaryotes. In *Microbiology Monography*; Shilvey, J. M., Ed.; Springer-Verlag: Berlin, Heidelberg, Germany, 2006; Vol. 2, pp 79–114. (b) Balaban, T. S.; Tamiaki, H.; Holzwarth, A. R. In *Supramolecular Dye Chemistry*; Würthner, F., Ed.; *Topics in Current Chemistry* 258; Springer-Verlag: Berlin, Heidelberg, Germany, 2005; pp 1–38. (c) Overmann, J.; Cypionka, H.; Pfennig, N. *Linnol. Oceanogr.* **1992**, *37*, 150–155. (d) Manske, A. K.; Glaeser, J.; Kuypers, M. M.; Overmann, J. *Appl. Environ. Microbiol.* **2005**, *71*, 8049–8060.
- (2) Beatty, J. T.; Overmann, J.; Lince, M. T.; Manske, A. K.; Lang, A. S.; Blankenship, R. E.; Van Dover, C. L.; Martison, T. A.; Plumley, F. G. *Proc. Natl. Acad. Sci. U.S.A.* **2005**, *102*, 9306–9310.
- (3) Blankenship, R. E. *Molecular Mechanisms of Photosynthesis*; Blackwell: Oxford, U.K., 2002.
- (4) (a) Staehelin, L. A.; Golecki, J. R.; Fuller, R. C.; Drews, G. *Arch. Mikrobiol.* **1978**, *119*, 269–277. (b) Staehelin, L. A.; Golecki, J. R.; Drews, G. *Biochim. Biophys. Acta* **1980**, *589*, 30–45.
- (5) (a) van Rossum, B.-J.; Steensgaard, D. B.; Mulder, F. M.; Boender, G.-J.; Schaffner, K.; Holzwarth, A. R.; de Groot, H. J. M. *Biochemistry* **2001**, *40*, 1587–1595. (b) Pšenčík, J.; Ikonen, T. P.; Laurinmäki, P.; Merckel, M. C.; Butcher, S. J.; Serimaa, R. E.; Tuma, R. *Biophys. J.* **2004**, *87*, 1165–1172. (c) Balaban, T. S. *Acc. Chem. Res.* **2005**, *38*, 612–623. (d) Pšenčík, J.; Arellano, J. B.; Ikonen, T. P.; Borrego, C. M.; Laurinmäki, P.; Butcher, S. J.; Serimaa, R. E.; Tuma, R. *Biophys. J.* **2006**, *91*, 1433–1440. (e) Ikonen, T. P.; Li, H.; Pšenčík, J.; Laurinmäki, P. A.; Butcher, S. J.; Frigaard, N.-F.; Serimaa, R. E.; Bryant, D. A.; Tuma, R. *Biophys. J.* **2007**, *93*, 620–628.
- (6) (a) Balaban, T. S.; Bhise, A. D.; Fischer, M.; Linke-Schaetzel, M.; Roussel, C.; Vanthuyne, N. *Angew. Chem., Int. Ed.* **2003**, *42*, 2140–2144. (b) Balaban, T. S.; Bhise, A. D.; Linke-Schaetzel, M.; Vanthuyne, N.; Roussel, C. *Eur. J. Org. Chem.* **2004**, 3919–3930.
- (7) (a) Shibata, R.; Tamiaki, H. *Bioorg. Med. Chem.* **2006**, *14*, 2235–2241. (b) Kunieda, M.; Tamiaki, H. *J. Org. Chem.* **2005**, *70*, 820–828. (c) Miyatake, T.; Shitasue, K.; Omori, Y.; Nakagawa, K.; Fujiwara, M.; Matsushita, T.; Tamiaki, H. *Photosynth. Res.* **2005**, *86*, 131–136. (d) Sasaki, S.; Omoda, M.; Tamiaki, H. *J. Photochem. Photobiol., A* **2004**, *162*, 307–315.
- (8) (a) Huber, V.; Katterle, M.; Lysetska, M.; Würthner, F. *Angew. Chem., Int. Ed.* **2005**, *44*, 3147–3151. (b) Röger, C.; Müller, M.; Lysetska, M.; Miloslavina, Y.; Holzwarth, A. R.; Würthner, F. *J. Am. Chem. Soc.* **2006**, *128*, 6542–6543.
- (9) Balaban, T. S.; Linke-Schaetzel, M.; Bhise, A. D.; Vanthuyne, N.; Roussel, C.; Anson, C. A.; Buth, G.; Eichhöfer, A.; Foster, K.; Garab, G.; Gliemann, H.; Goddard, R.; Javorfi, T.; Powell, A. K.; Rösner, H.; Schimmel, Th. *Chem.-Eur. J.* **2005**, *11*, 2267–2275.
- (10) Balaban, T. S.; Goddard, R.; Linke-Schaetzel, M.; Lehn, J.-M. *J. Am. Chem. Soc.* **2003**, *125*, 4233–4239.
- (11) Sheldrick, G. M. *SHELX-97, Program for X-ray crystal structure determination and refinement*; Göttingen University: Göttingen, Germany, 1997.
- (12) Brandenburg, K. *Diamond*, version 3.0; Crystal Impact GbR: Bonn, Germany, 2004.
- (13) Balaban, M. C.; Balaban, T. S. *J. Porphyrins Phthalocyanines* **2007**, *11*, 277–286.
- (14) (a) Jin, F.; Confalone, P. N. *Tetrahedron Lett.* **2000**, *41*, 3271–3273. (b) Takanami, T.; Hayashi, M.; Chijimatsu, H.; Inoue, W.; Suda, K. *Org. Lett.* **2005**, *7*, 3937–3940. (c) Cottyn, B.; Vichard, D.; Terrier, F.; Nioche, P.; Raman, C. S. *Synlett* **2007**, 1203–1206.
- (15) Arnold, D. P.; Bott, R. C.; Eldridge, H.; Elms, F. M.; Smith, G.; Zojaji, M. *Aust. J. Chem.* **1997**, *50*, 495–503.
- (16) (a) Takagi, K.; Okamoto, T.; Sakakibara, Y.; Ohno, A.; Oka, S.; Hayama, N. *Bull. Chem. Soc. Jpn.* **1976**, *49*, 3177–3180. (b) Schareina, T.; Zapf, A.; Beller, M. *J. Organomet. Chem.* **2004**, *689*, 4576–4583.
- (17) Stazi, F.; Palmisano, G.; Turconi, M.; Santagostino, M. *Tetrahedron Lett.* **2005**, *46*, 1815–1818.
- (18) Shibano, Y.; Umeyama, T.; Matano, Y.; Imahori, H. *Org. Lett.* **2007**, *9*, 1971–1974.
- (19) (a) Suslick, K. S.; Chen, C.-T.; Meredith, G. R. *J. Am. Chem. Soc.* **1992**, *114*, 6928–6930. (b) Priyadarshy, S.; Therien, M. J.; Beratan, D. N. *J. Am. Chem. Soc.* **1996**, *118*, 1504–1510. (c) LeCours, S. M.; Guan, H.-W.; DiMaggio, S. G.; Wang, C. H.; Therien, M. J. *J. Am. Chem. Soc.* **1996**, *118*, 1497–1503. (d) Yueng, M.; Ng, A. C. H.; Drew, M. G. B.; Vorpagel, E.; Breitung, E. M.; McMahon, R. J.; Ng, D. K. P. *J. Org. Chem.*, **1998**, *63*, 7143–7150. (e) Chou, J. H.; Kosal, M. E.; Nalwa, H. S.; Rakow, N. A.; Suslick, K. S. In *The Porphyrin Handbook*; Kadish, K. M., Smith, K. M., Guillard, R., Eds.; Academic Press: San Diego, CA, 1999; Vol. 6, Chapter 41, pp 53–58. (f) Ma, T.; Inoue, K.; Noma, H.; Yao, K.; Abe, E. *J. Photochem. Photobiol., A* **2002**, *152*, 207–212. (g) Monnerau, C.; Blart, E.; Montebault, V.; Fontaine, L.; Odobel, F. *Tetrahedron* **2005**, *61*, 10113–10121. (h) Ray, P. C.; Leszczynski, J. *Chem. Phys. Lett.* **2006**, *419*, 578–583. (i) Ray, P. C.; Sainudeen, Z. *J. Phys. Chem. A* **2006**, *110*, 12342–12347. (j) Notaras, E. G. A.; Fazekas, M.; Doyle, J. J.; Blau, W. J.; Senge, M. O. *Chem. Commun.* **2007**, 2166–2168.
- (20) Rappoport, D.; Furche, F. *J. Am. Chem. Soc.* **2004**, *126*, 1277–1284 and further references therein.
- (21) (a) Hartwig, J. F.; Kawatsura, M.; Hauck, S. I.; Shaughnessy, K. H.; Alcazar-Roman, L. M. *J. Org. Chem.* **1999**, *64*, 5575–5580. (b) Hooper, M. W.; Utsunomiya, M.; Hartwig, J. F. *J. Org. Chem.* **2003**, *68*, 2861–2873. (c) Takanami, T.; Hayashi, M.; Hino, F.; Suda, K. *Tetrahedron Lett.* **2003**, *44*, 7353–7357. (d) Esdaile, L.; Senge, M. O.; Arnold, D. P. *Chem. Commun.* **2006**, 4192–4194.
- (22) Liu, C.; Shen, D.-M.; Chen, Q.-Y. *J. Org. Chem.* **2007**, *72*, 2732–2736.
- (23) (a) Deans, R.; Kim, J.; Machacek, M. R.; Swager, T. M. *J. Am. Chem. Soc.* **2000**, *122*, 8565–8566. (b) Luo, J.; Xie, Z.; Lam, J. W. Y.; Cheng, L.; Chen, H.; Qiu, C.; Kwok, H. S.; Zhan, X.; Liu, X.; Zhu, D.; Tang, B. Z. *Chem. Commun.* **2001**, 1740–1741. (c) An, B.-K.; Kwon, S.-K.; Jung, S.-D.; Park, S. Y. *J. Am. Chem. Soc.* **2002**, *124*, 14410–14415. (d) Bhongale, C. J.; Chang, C.-W.; Diau, E. W.-G.; Hsu, C.-S.; Dong, Y.; Tang, B.-Z. *Chem. Phys. Lett.* **2006**, *419*, 444–449.
- (24) Huijser, A.; Marek, P. L.; Savenije, T. J.; Siebbeles, L. D. A.; Scherer, T.; Hauschild, R.; Szymkowski, J.; Kalt, H.; Hahn, H.; Balaban, T. S. *J. Phys. Chem. C* **2007**, *111*, 11726–11733.
- (25) (a) Brookfield, R. L.; Ellul, H.; Harriman, A.; Porter, G. *J. Chem. Soc., Faraday Trans. 2* **1986**, *82*, 219–233. (b) Hsiao, J.-S.; Krueger, B. P.; Wagner, R. W.; Johnson, T. E.; Delaney, J. K.; Mauzerall, D. C.; Fleming, G. R.; Lindsey, J. S.; Bocian, D. F.; Donohoe, R. J. *J. Am. Chem. Soc.* **1996**, *118*, 11181–11193. (c) Van, Patten, P. G.; Shreve, A. P.; Lindsey, J. S.; Donohoe, R. J. *J. Chem. Phys. B* **1998**, *102*, 4209–4216. (d) Nakano, A.; Osuka, A.; Yamazaki, I.; Yamazaki, T.; Nishimura, Y. *Angew. Chem., Int. Ed. Engl.* **1998**, *37*, 3023–3027. (e) Brodard, P.; Matzinger, S.; Vauthey, E.; Mongin, O.; Papamichael, C.; Gossauer, A. *J. Phys. Chem. A* **1999**, *103*, 5858–5870. (f) Cho, H. S.; Song, N. W.; Kim, Y. H.; Jeoung, S. C.; Hahn, S.; Kim, D.; Kim, S. K.; Yoshida, N.; Osuka, A. *J. Phys. Chem. A* **2000**, *104*, 3287–3298. (g) Ha, J.-H.; Cho, H. S.; Song, J. K.; Kim, D.; Aratani, N.; Osuka, A. *Chem. Phys. Chem.* **2004**, *5*, 57–67. (h) Nakamura, Y.; Hwang, I.-W.; Aratani, N.; Ahn, T. K.; Ko, D. M.; Takagi, A.; Kawai, T.; Matsumoto, T.; Kim, D.; Osuka, A. *J. Am. Chem. Soc.* **2005**, *127*, 236–246.
- (26) (a) Harriman, A.; Magda, D. J.; Sessler, J. L. *J. Chem. Soc., Chem. Commun.* **1991**, 345–348. (b) Harriman, A.; Magda, D. J.; Sessler, J. L. *J. Phys. Chem.* **1991**, *95*, 1530–1532. (c) Sessler, J. L.; Magda, D.; Furuta, H. *J. Org. Chem.* **1992**, *57*, 818–826. (d) Hajjaj, F.; Yoon, Z. S.; Yoon, M.-C.; Park, J.; Satake, A.; Kim, D.; Kobuke, Y. *J. Am. Chem. Soc.* **2006**, *128*, 4612–4623. (e) Kobuke, Y. *Eur. J. Inorg. Chem.* **2006**, 2333–2351. (f) Balaban, T. S.; Berova, N.; Drain, C. M.; Hauschild, R.; Huang, X.; Kalt, H.; Lebedkin, S.; Lehn, J.-M.; Nifaitis, F.; Pescitelli, G.; Prokhorenko, V. I.; Riedel, G.; Smeureanu, G.; Zeller, J. *Chem.-Eur. J.* **2007**, *13*, 8411–8427.
- (27) Hunter, C. A.; Sanders, J. K. M. *J. Am. Chem. Soc.* **1990**, *112*, 5525–5534.
- (28) (a) Balaban, T. S.; Holzwarth, A. R.; Schaffner, K.; Boender, G.-J.; de Groot, H. J. M. *Biochemistry*, **1995**, *34*, 15259–15266. (b) Egawa, A.; Fujiwara, T.; Mizoguchi, T.; Kakitani, Y.; Koyama, Y.; Akutsu, H. *Proc. Natl. Acad. Sci. U.S.A.* **2007**, *104*, 790–795.
- (29) (a) Dähne, L. *J. Am. Chem. Soc.* **1995**, *117*, 12855–12860. (b) Wang, M.; Silva, G. L.; Armitage, B. A. *J. Am. Chem. Soc.* **2000**, *122*, 9977–9986. (c) Dautel, O. J.; Wantz, G.; Almayrac, R.; Flot, D.; Hirsch, L.; Lere-Porte, J.-P.; Parneix, J.-P.; Serein-Spirau, F.; Vignau, L.; Moreau, J. E. *J. Am. Chem. Soc.* **2006**, *128*, 4892–4901.
- (30) Desiraju, G. R. *Angew. Chem., Int. Ed.* **2007**, *46*, 8342–8356.